Chapter 4

# Applications of Nanostructural NiTi Alloys for Medical Devices

Elena O. Nasakina, Mikhail A. Sevostyanov, Alexander S. Baikin, Alexey V. Seryogin, Sergey V. Konushkin, Konstantin V. Sergienko, Alexander V. Leonov and Alexey G. Kolmakov

Additional information is available at the end of the chapter

http://dx.doi.org/10.5772/intechopen.69238

**Abstract**

New nanostructural shape memory alloy (55.91 wt% of Ni and 44.03 wt% of Ti) for the production of minimally invasive implantation medical devices (stents) was tested for corrosion resistance under static conditions by dipping it into solutions with various acidities (pH from 1.68 to 9.18) for 2 years, for static mechanical properties and for biocompatibility. The material for investigations was 280-μm wires before and after thermal treatment at 450°C for 15 min in air and surface mechanical treatment. The characteristic image and size of grains were determined using the transmission electron microscope (TEM), and the phase composition; surface morphology; and the layer-by-layer composition were investigated using an X-ray diffractometer; a scanning electron microscope (SEM); and an Auger spectrometer. The nickel release from the investigated nanostructural nitinol is less in comparison with data for microstructural nitinol in a solution of any acidity. Dissolution in the alkali medium is absent. A significant retardation of the nickel ion release (and insignificant concentration as a whole) and the absence of titanium ion release in the weakly acidic and neutral solutions with polished samples are observed. A simultaneous 7–11% increase in strength and plasticity in comparison with microstructural nitinol was attained. Toxicity of samples has not been revealed.

**Keywords:** nitinol, biocompatibility, corrosion resistance, shape memory effect, superelasticity

## 1. Introduction

Nitinol (NiTi) alloys possessing a shape memory effect (SME) and mechanical characteristics similar to the behavior of living tissues have been already used for years as the material for production of medical devices, including implants, for example stents [1–6].

SME promotes the production of the least traumatic self-expanding stents, which are implanted into the human body to relieve obstruction or constriction of the respiratory, digestive, excretory, and cardiovascular systems and to restore the normal circulation of physiological flows without the need for additional devices except the catheter carrier [6]. But nitinol contains nickel (including on its surface) which is toxic for organisms [7–9]. Different authors give completely different durations (up to constant) and magnitudes (from fractions to hundreds of mg/L) of the nickel ion release from microstructural nitinol into the medium [8–16]. And also, a different level of nitinol biocompatibility and of its electro-chemical corrosion characteristics is noted [2, 8–10, 17, 18]. Nitinol properties are generally determined by the structure and the composition, which depend on the production process and treatments [2, 8–9, 11, 17, 19–22].

As is well known, formation of nanostructures imparts special, controlled characteristics to materials [23, 24]. Nitinol, as titanium, is a self-passivated material, that is, it forms a complex surface oxide layer, which protects the material from corrosion, and also is biocompatible in itself [2, 10–12]. This oxide layer also surrounds each grain. Therefore, it is possible to assume that increase in a volume fraction of such grain boundaries in alloy at its nanostructuring will positively affect its corrosion resistance and biocompatibility. On the other hand, the high density of intergranular surface defects could lead to a poor corrosion performance since corrosion attack typically initiates at surface heterogeneities [25].

As described in Ref. [25], one of the most efficient methods of fabrication of bulk nanocrystalline materials is the severe plastic deformation (SPD) leading to the breakdown of coarse grains into nanosized (with the size less than 100 nm) grains. The main SPD techniques are equal channel angular extrusion (ECAP) including thermomechanical treatment, high pressure torsion (HPT), hydrostatic extrusion, and others.

It is noticed in literature that nanostructure has an ambiguous effect on the nitinol properties and this is little studied. Investigations showed that in HCl nitinol in the nanosized state (grain diameter of 10 nm) reveals a significantly lower corrosion resistance than in the microstructural state because of an increase in the boundary length and in the amount of defects of the grain structure; and nitinol in NaCl, on the contrary, is more passive (consequently corrosion resistant) [26]. In the study [25, 27–29], there is no difference in corrosion processes between micro- and nanostructured nitinol. But in case of nanostructured titanium, corrosion resistance reduction was observed [30] though in all works positive influence on mechanical properties of materials was noted. In Refs. [31–33], large recoverable strains, resistance against cyclic plasticity mechanisms, plasticity, and good fatigue response were achieved by grain refinement by means of ECAP. HPT produced an ultrafine-grained structure with grain sizes in the range from 5 to 100 nm, which leads to a very high strength, good ductility, high recovery stress, and to a maximum reverse strain, significantly improving cyclic endurance and pseudoelasticity [34]. Additional electropulse current treatment of coarse-grained

and ultrafine-grained NiTi (grain diameter more than 100 nm) results in the formation of structures with a grain size less than 80 and 100 nm, correspondingly (was more effective for microstructural material), with increased deformability and mechanical properties [35]. At the same time, according to the computational model and the experimental data in Ref. [36], it was shown that when the grain size is smaller than some critical value (around 50–80 nm in all directions), the martensitic phase transformation is totally suppressed even though the material severely deforms; whereas in another experiment, nanostructure does not prevent phase transformations that are influenced only by aging regime and cooling rate [37]. Authors of Ref. [38] noted that the cold-drawn nitinol contains 50 nm thick grains and possesses quite high tensile strength, hardness, and fatigue life, the maxima of which are reached after heat treatments at 450°C within 15 min; and heat treatments at above 450°C induced recrystallization and grain and precipitate growth. It is shown that the nanostructural morphology of the nitinol and titanium surfaces at the tissue-implant interface positively affects biocompatibility *in vitro* and *in vivo* and enhances functional activity of desirable cell cultures and enzymes without any fibrous tissue intervention. However, not all nanomorphologies on implants imparted a similar biological response [39, 40].

Thus, it is still of interest how nanostructuring can influence operational characteristics of nitinol as a medical (implantation) material. The aim of this chapter is to investigate the composition, structure, and properties of polycrystalline nitinol with nanograins.

## 2. Obtaining and investigating nanostructural NiTi alloy for medical application

Nanostructured wires with a diameter of 280 μm made of nitinol (50.9 wt% of Ni) were obtained from the Institution of Russian Academy of Sciences, A.A. Baikov Institute of Metallurgy and Material Science, before processing and after mechanical and/or thermal treatments were investigated.

To obtain the material, we used the modernized complex plastic deformation technology developed in the IMET RAS. The corresponding charge was re-melted several times in a vacuum furnace in argon. Ingots were transformed by rolling and rotary forging at a temperature of 750–1000°C into bars with a diameter of up to 4 mm, from which the wire was obtained by step-wise hot drawing through a synthetic diamond die and by intermediate thermal treatment for stabilization of the material structure and removal of mechanical stress.

The mechanical treatment (by abrasive paper from 180 to 1000 grit and finally by GOI (State Optical Institute) paste to a mirror surface) of the wire surface was carried out by an abrasive cloth for the removal of flat indentations and defects in the form of dimples after wire drawing. The decrease in the diameter was to 10 μm in comparison with the original. The thermal treatment of nitinol that allows one to vary static properties and cyclic loadings in operating conditions with a wide range of deformations is extremely important for stabilization of the properties, constraining (shaping) the samples, and successful application of the product. The optimal conditions for the thermal treatment were chosen from the previous researches as

*T* = 450°C and an annealing time of 15 min (what has coincided with [38]), and carried out in a LOIP LF 7/13_G2 muffler (Russia) equipped with a programmed controller.

To investigate the wire microstructure, the preliminary etching of the surface was carried out in a mixture of 1 mL HF + 2 mL $HNO_3$ + 47 mL $H_2O$ composition for 2–3 min, upon termination of which the sample was washed several times in distilled water and dried in air. Investigations were carried out on an Axiovert 40 MAT optical metallographic microscope (Carl Zeiss, Germany) with digital image processing. The characteristic image and size of grains were determined with the use of a TECNAI 12 transmission electron microscope (TEM) (FEI COMPANY, USA), and samples were prepared by means of a GATAN 691 ion-etching device (Gatan Inc., USA). To determine the phase composition, we used an Ultima IV X-ray diffractometer (Rigaku Co., Japan) in Cu K$\alpha$—radiation on the basis of Bragg-Brentano method. Phase analysis was prepared in the PDXL program complex using the ICDD database. The surface morphology and the layer-by-layer composition were investigated on a scanning election microscope (SEM) VEGA II SBU with the module INCA Energy for energy-dispersive analysis (TESCAN, Czech Republic) and on a JAMP-9500F Auger spectrometer (JEOL Co., Japan) in combination with ion etching at argon bombardment under an angle of 30°.

The bright-field TEM image in **Figure 1a** shows that nitinol grains resemble nanofibers with a cross-section size from 30 to 70 nm, and the longitudinal section size of fibers is several microns. Thus, grains are extended along the wire axis. Rings are seen in the microdiffraction pattern (**Figure 1b**), which point to polycrystalline structure of the sample. The calculation and analysis of the interplanar spacing distances from the electron diffraction patterns show that they correspond to the B2 phase.

Also, according to the energy-dispersive and X-ray structural analyses (**Figure 2a**), the material volume is represented by the base of the B2 phase of TiNi and inclusions of $Ti_2Ni$

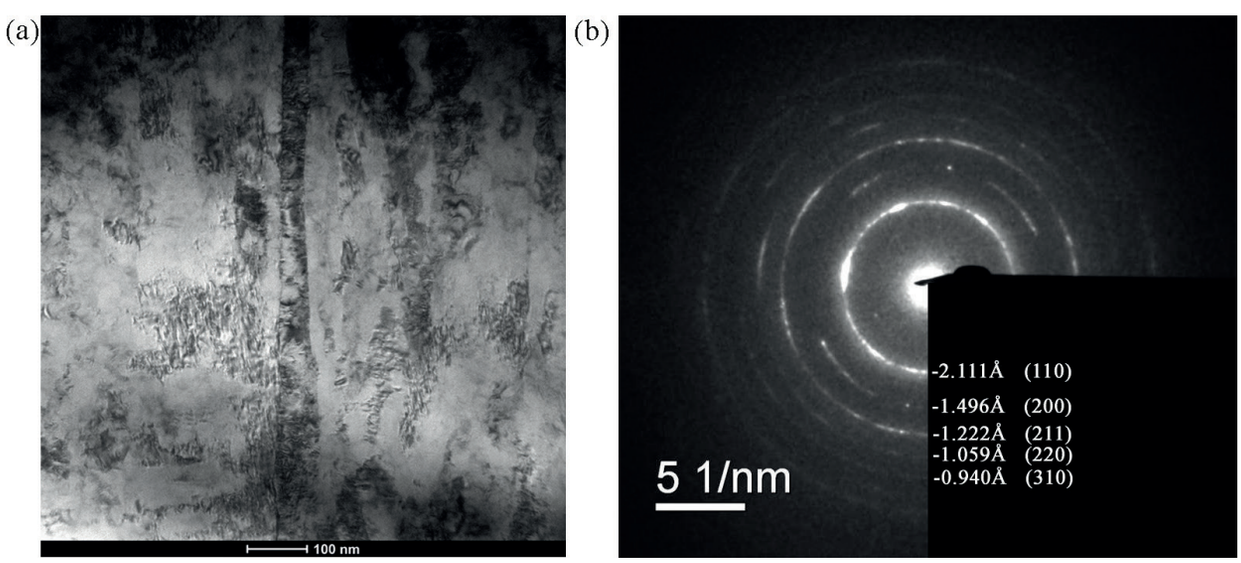


**Figure 1.** Transmission electron microscopy data: (a) bright-field TEM image and (b) microdiffraction pattern.

http://dx.doi.org/10.5772/intechopen.69238

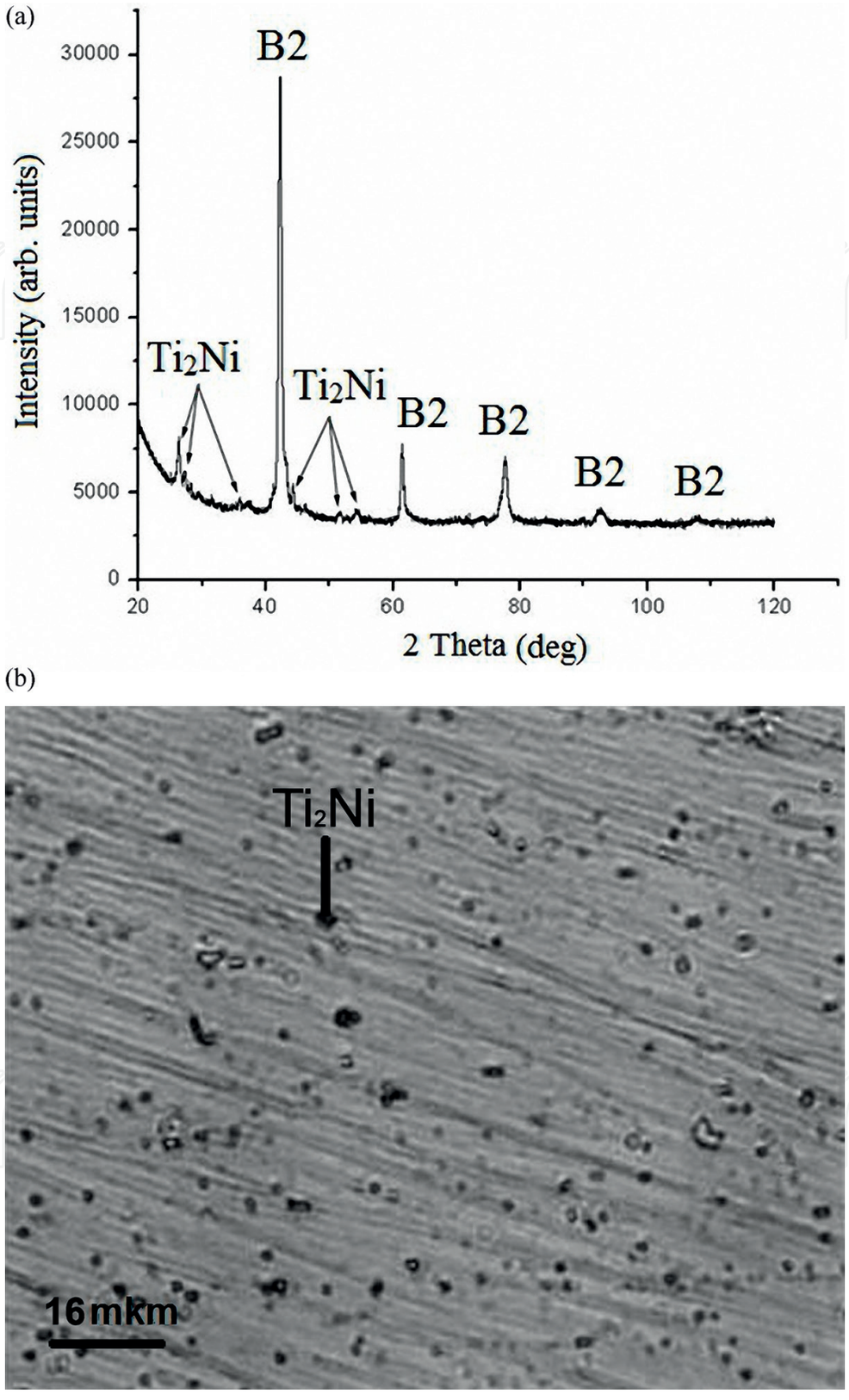


**Figure 2.** Nitinol structure data: (a) X-ray diffraction patterns and (b) microstructure analysis.

intermetallides. The character of X-ray patterns indicates that the composition is unchanged after thermal treatment. The microstructure analysis (**Figure 2b**) verifies that the base of the alloy investigated is represented by the B2 phase, and the material contains $Ti_2Ni$ intermetallides, and the sizes and the volume fraction of which are unchanged after annealing.

According to the SEM images (**Figure 3a**), the wire surface before treatment is heterogeneous and covered by spots, dark areas alternating with bright ones and the high roughness is clearly expressed. After annealing (**Figure 3b**), the surface externally is similar to the initial one, whereas after polishing (**Figure 3c**) practically all defects and the roughness are smoothed, spots are absent, and only traces of treatment are visible. Surface microdefects are grooves with a depth and width of less than 1 μm, and after polishing and annealing, the wire surface is the most-smoothed and uniform (**Figure 3d**).

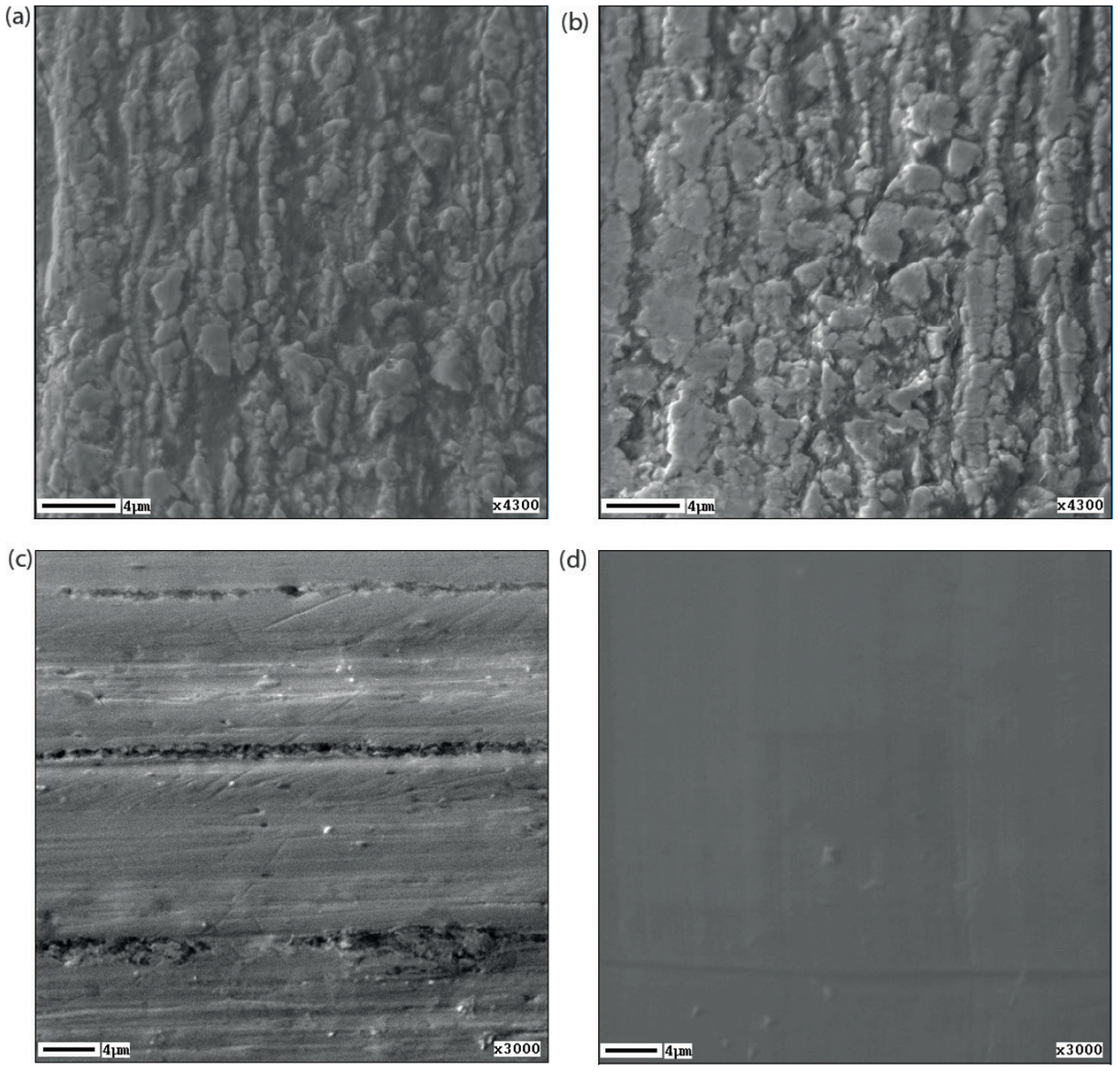


**Figure 3.** SEM image of the wire surface: (a) before treatment, (b) after annealing, (c) after polishing, and (d) after polishing and annealing.

The compositions of bright and dark spots are different (**Figure 4a**): a high content of titanium oxide is revealed in bright ones and carbon, in dark ones. Both layers attain 3 μm in thickness and are not placed over each other. Such a thick surface layer, as was believed, was a result of the long intermediate thermal treatment during the wire production [8, 9, 41]. Most likely, therefore, annealing for 15 min does not have an effect on features of changing the composition. Carbon is present on the wire surface, probably, due to graphite-containing lubricant (used during wire drawing), which remains on the wire surface and then sticks during annealing. The same effect (impurities on the surface after several cycles of treatment due to lubricant) was observed in Ref. [11]. The composition of the polished surface is homogeneous (**Figure 4b**): the entire wire is covered by an oxide layer less than 20 nm in thickness, which, according to the literature [41], must positively affect corrosion resistance under dynamic conditions because thin oxide layers show greater flexibility and may adapt to loads applied to the material. The minus is the presence of nickel in the surface layer, though in an insignificant amount. The subsequent annealing promotes the formation of an oxide-nitride layer up to 80–150 nm in depth, to 50–60 nm free from nickel that could affect corrosion resistance of material positively (**Figure 4c**), that is also connected with thermal treatment which leads to the formation of mixed surface layer consisting of titanium and nickel oxides and to the growth of the oxide layer thickness [8, 9, 41].

The mechanical properties of samples with a working part length of 45 mm were determined under the conditions of static stretching on an Instron 3382 (Instron, USA) universal testing machine with a loading speed of 2 mm/min. The base diameter was used in the calculation of strength properties. Three to five samples were tested per one experimental point. The conventional yield strength $\sigma_{0.2}$, the ultimate strength $\sigma_u$, and the relative elongation $\delta$ were determined (**Table 1**).

Results of the mechanical stretching tests showed positive influence of annealing on strength properties of alloy in both structural states, and strength properties of a nanostructural nitinol exceeded strength properties of microstructural nitinol by 1.3–1.5 times. Nitinol wire polishing after drawing promotes an increase in the static properties of a nanostructural alloy of 18%. Relative elongations of all samples were of 51–53%.

Heat treatment significantly increases cyclic durability of nanostructural material (**Figure 5**). Its durability in the initial state is insignificant, and all fatigue curves lie in the low-cyclic area (below $N = 6 \times 10^3$ cycles). After annealing, durability sharply increases both in the field of low-cycle and multicycle fatigue. The durability limit after annealing on the basis of $4 \times 10^6$ cycles is 400 MPa.

The wire disintegrates with the formation of a neck (**Figure 6**). The fracture surface is aligned almost perpendicularly to the stretching axis. It consists of a set of unequally sized self-similar pores (cups) of the viscous break. The destruction starts from the most serious defects on the sample surface in the zone of the neck where the main crosscut crack, to which the formed pores are merged, is formed. Heat treatment practically does not influence the nature of destruction.

Micro-Vickers hardness measurements determined at loading 1–2 N by the WOLPERT GROUP 401/402 device—MVD (WILSON Instruments, USA) equipped with a light microscope.

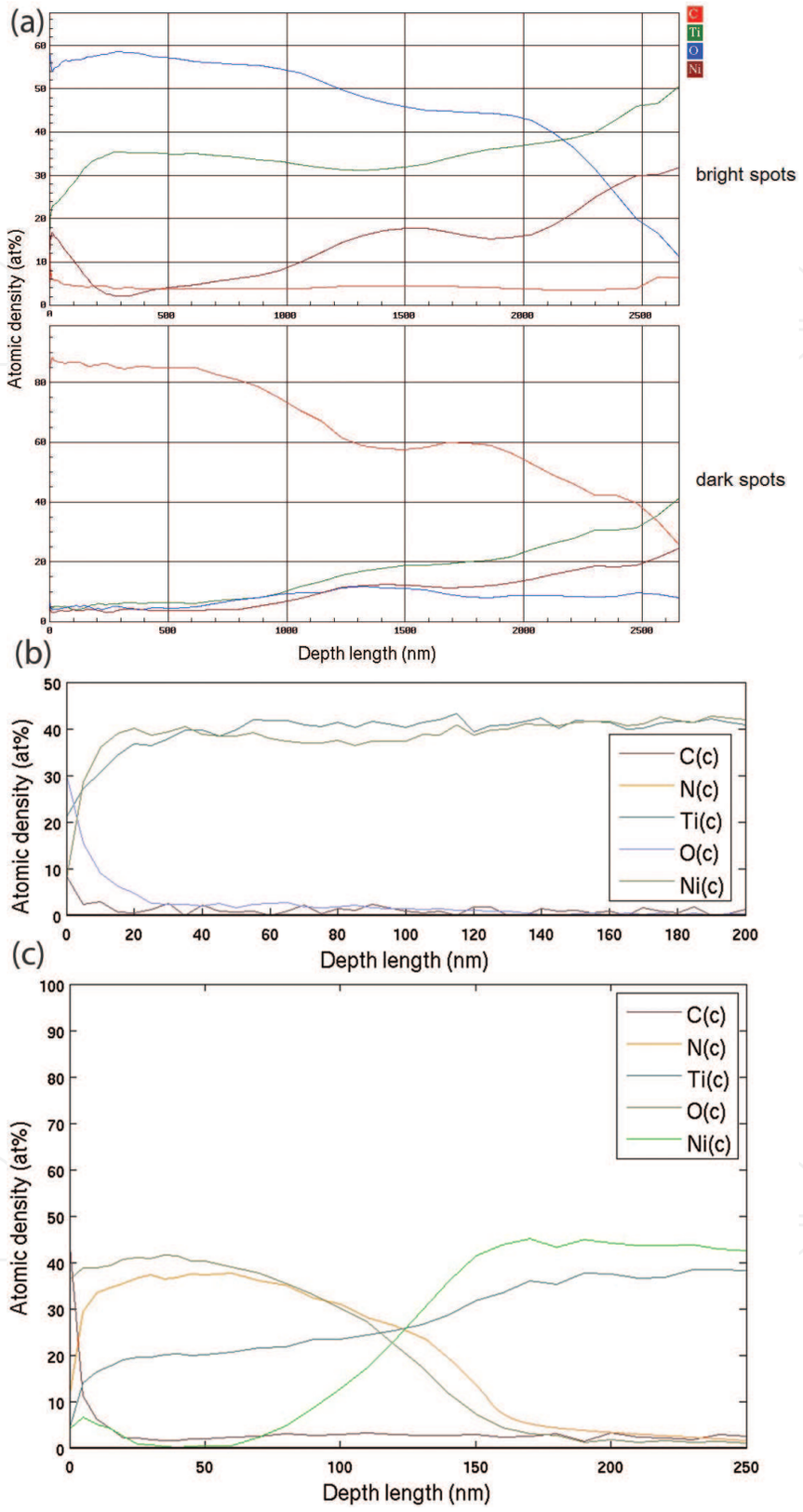


**Figure 4.** Wire surface structure according to Auger spectroscopy prior to the immersion testing: (a) before treatment and after annealing (dark and bright spots in **Figure 3a** and **b**), (b) after polishing, and (c) after polishing and annealing.

| Batch number | Sample | $\sigma_{0.2}$, MPa | $\sigma_u$, MPa |
|---|---|---|---|
| 1 | Microstructural nitinol before treatment | 497 | 1423 |
| 2 | Nanostructural nitinol before treatment | 507 | 1485 |
| 3 | Microstructural nitinol, annealing of 450°C, 15 min | 564 | 1635 |
| 4 | Nanostructural nitinol, annealing of 450°C, 15 min | 742 | 1885 |

**Table 1.** Effect of annealing on nitinol mechanical properties.

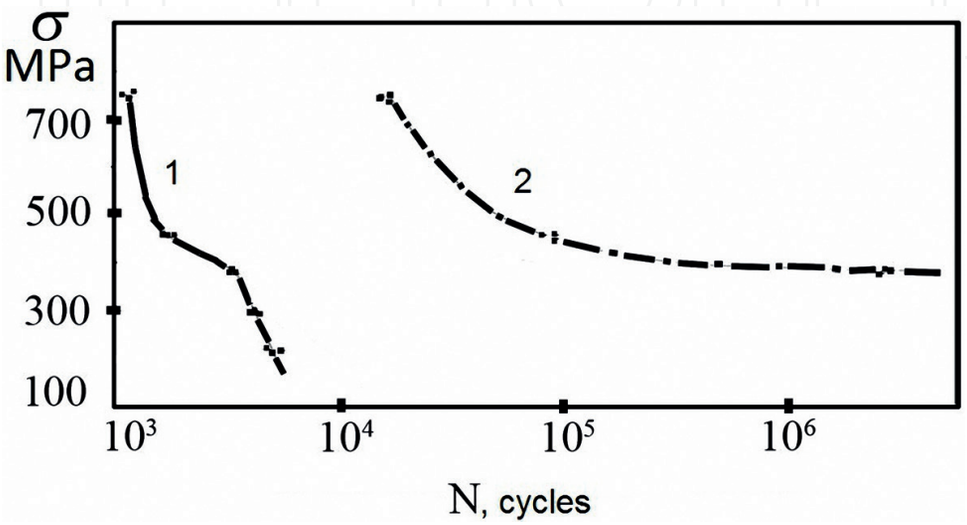


**Figure 5.** Fatigue curves of a nanostructural nitinol before treatment (1) and after annealing at 450°C, 15 min (2).

Microhardness of nanostructural material is higher by ≈ 38% in comparison with a microstructural analog (332 ± 3 and 240 ± 3 HV, respectively). It can be explained by the increase in volume fraction of grain boundaries and also by the presence of titanium oxides on these borders, the hardness of which is higher than the basic hardness. As a result of surface polishing, a formation of a thin uniform oxide layer with a small share of impurity takes place, and microhardness increases by 17.5% (from 332 ± 3 to 390 ± 4 HV). The subsequent annealing within 15 min at 450°C promotes the thickening of the oxide layer and an increase in the share of titanium oxides in it that leads to additional increase in microhardness by 2.3% (to 399 ± 3 HV).

The corrosion resistance of the material was determined under static conditions by immersion into solutions with various acidities because pH in the human body changes from 1 to 9 (for example, 1.05 at the duodenum; 1.53–1.67 is the norm of gastric juice; 3.8–4 in the near-surface area of the bowels; 7.34–7.43 is the norm of blood; 8.5–9 in the bowels; etc.). We used a neutral 0.9 wt% solution of sodium chloride, artificial plasma, and four standard buffer solutions (to reproduce acidic and alkaline media at the given level) [8, 9, 42], which are listed in **Table 2**, and for comparison, we also used a 0.03-M solution of hydrochloric acid. The standard buffer solutions were prepared from corresponding standard trimetric substances (fixanals) made by Merk (USA).

Wire samples (1—TiNi before treatment, 2—TiNi after annealing, 3—TiNi after polishing, and 4—TiNi after polishing and annealing), with a weight of 32.6 mg each (separately from

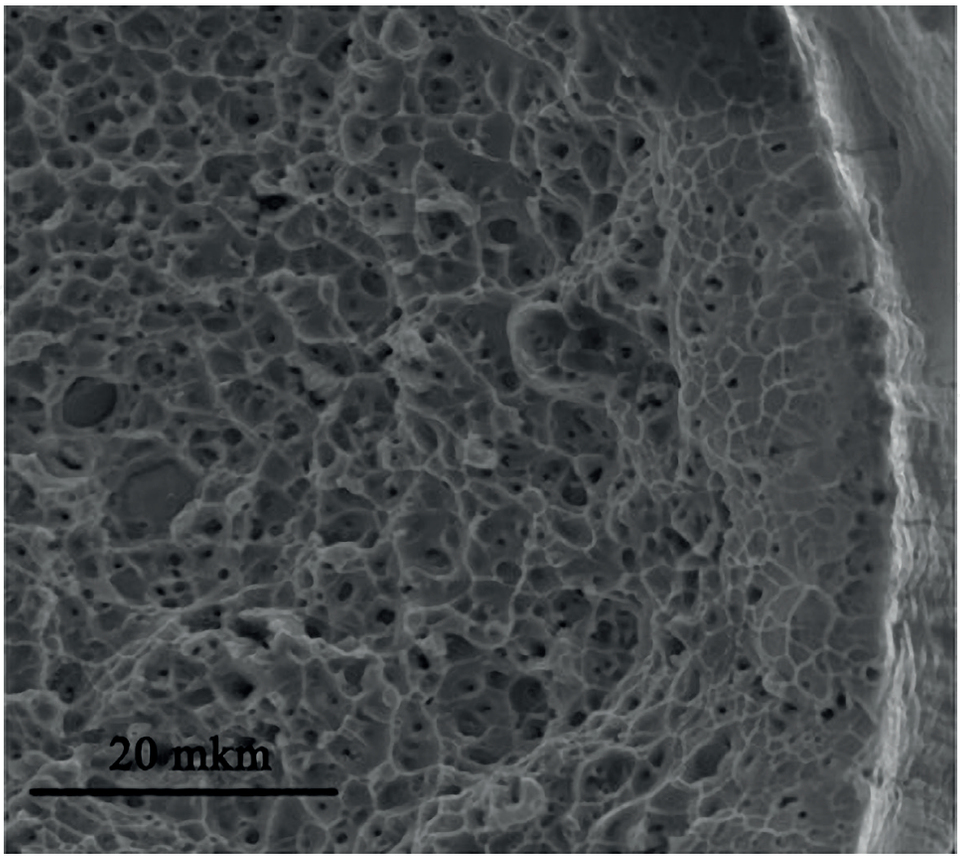


**Figure 6.** Disintegration behavior of the nitinol wire at static stretching.

| No | pH | Composition |
|---|---|---|
| 1 | 1.68 | Potassium tetraoxalate $KH_3C_4O_8 \times 2H_2O$, 0.05 M |
| 2 | 3.56 | Acid potassium tartrate $C_4H_5O_6K$, 0.025 M |
| 3 | 4.01 | Acid potassium phthalate $C_8H_5O_4K$, 0.05 M |
| 4 | 6.31 | Sodium chloride NaCl, 0.9 wt% |
| 5 | 9.18 | Acid sodium tetraborate $Na_2B_4O_7 \times 10H_2O$, 0.05 M |
| 6 | 7.36 | Artificial plasma: NaCl (92.3 mM), $NaHCO_3$ (26.3 mM), $K_2HPO_4$ (0.9 mM), KCl (2.7 mM), $NaH_2PO_4$ (0.22 mM), $CaCl_2$ (2.5 mM), $MgSO_4 \cdot 7H_2O$ (0.82 mM), $Na_2SO_4$ (1.48 mM), D-glucose $C_6H_{12}O_6$ (5.55 mM) [8–9] |

**Table 2.** pH and composition of the solutions used for immersion tests.

each other) were placed into flasks of heat-resistant laboratory glass (acidic and neutral media) or polypropylene (alkali medium) with 100 mL of the selected solution. The flasks were hermetically closed by a lapped cover and aged in a dark place. Sampling from flasks for analysis was done after a selected period (10, 25, 45, 60, 75, 236 or 287, 704, or 754 days). The initial buffer solutions were used as reference solutions. Analysis was carried out by an ULTIMA 2 sequential atomic emission spectrometry (HORIBA Jobin Yvon, Japan) for using atomic emission spectrometry (AES) with inductively coupled plasma (ICP) for direct simultaneous determination of titanium and nickel in solutions.

After immersion, the surface morphology and layer-by-layer composition were also investigated.

The results of measuring the ion release into solutions are represented in **Figures 7** and **8**. Insignificant corrosion is observed in acidic and neutral media, and the nickel concentration is less than the average magnitudes cited in the literature [8, 9, 11–13, 43]; however, the titanium content is revealed in solutions. There are no results about all samples in the alkaline environment and artificial plasma, and also about TiNi-3 and TiNi-4 samples in solutions with acidity 3.56–6.31 since, in these cases, the release of elements was zero or below a limit of detection for the overall time of the investigation.

Comparison of the treatment effect on the corrosion resistance of samples (**Figure 7**) makes it possible to conclude that the samples undergo the most corrosion after annealing, and the mechanical treatment, as was expected, strongly increases the corrosion resistance of nitinol.

According to the literature, the thermal treatment at a temperature from 400 to 1000°C, which is required for stabilization of the mechanical properties, always results in the significant worsening of the corrosion resistance due to the formation of nonuniform surface layers consisting of titanium and nickel oxides [21, 22, 41]. The undesirable effect of the thermal treatment on the corrosion resistance can also be explained by the occurrence of tempering and recrystallization of the outer cold-hardened (strengthening) layer on the surface of untreated nitinol, which forms during its production. At the same time, the surface treatment, which facilitates the formation of the most perfect and homogeneous passive film, increases the corrosion resistance.

And in case of TiNi-4 and TiNi-3 samples on an initial stage of researches regularity has the return nature. It is possible to assume that in the beginning thicker oxide surface layer of a sample after polishing and annealing acts as the better barrier against diffusion of nickel ions in solution;

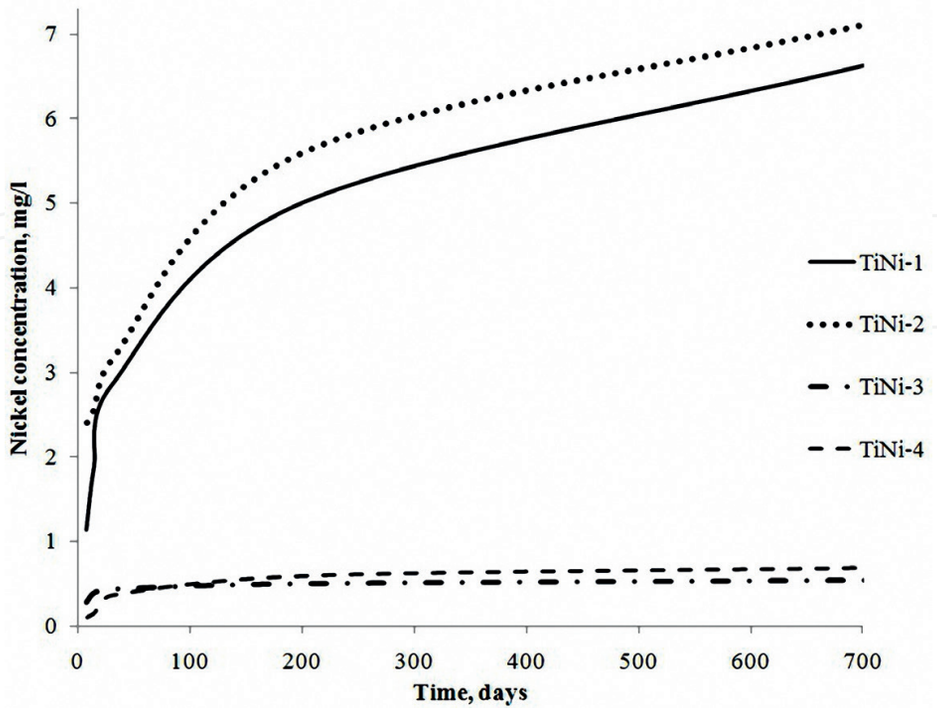


**Figure 7.** Nickel concentration in solution with pH 1.68 as a function of sample treatment and immersion time.

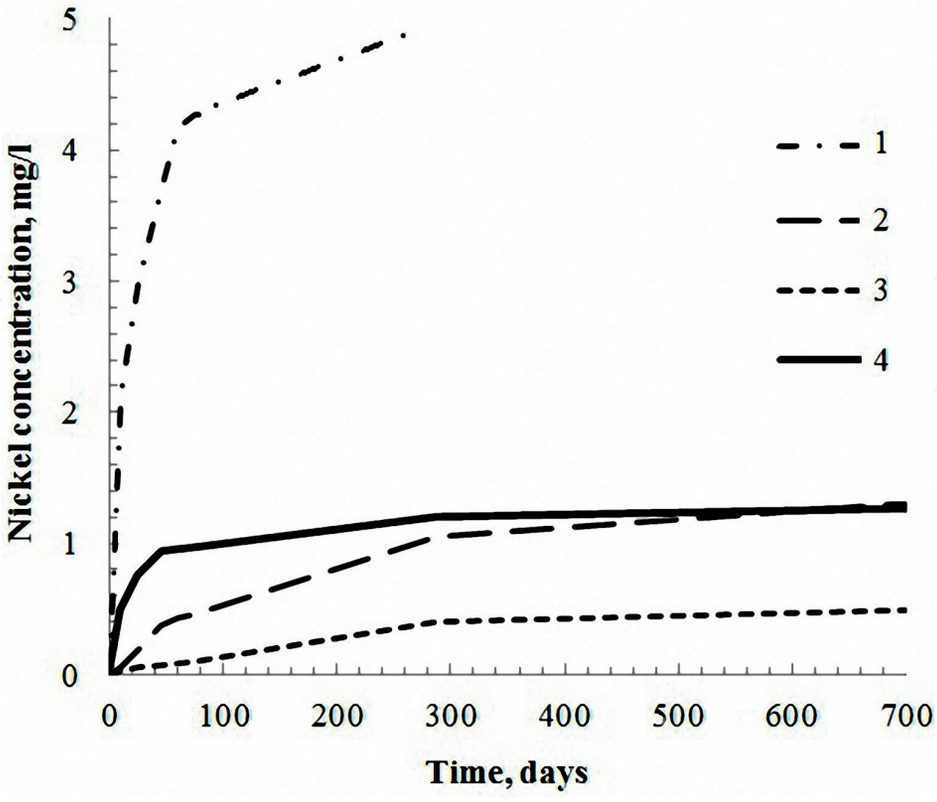


**Figure 8.** Nickel concentration in investigated solutions with various acidities with nitinol sample without treatment as a function of sampling time. The marked curves correspond to solution pH: 1—1.68, 2—3.56, 3—4.01, and 4—6.31.

however, after a long period of immersion, its nonuniformity does not allow to slow down leaching of elements as effectively as in case of a more uniform passive film which is initially received when polishing. The ratio of metal concentration in solutions with the annealed and the nonannealed samples at existence and lack of polishing treatment approximately coincides.

The surface examination after holding in solutions also reveals the hardest corrosive attack after annealing and the lowest after polishing. However, the wire diameter changes disproportionately to the ion concentration in the solution. For example, the diameters of untreated and annealed wires are almost equal after holding in the media with pH 1.68 (**Table 3**); that is, the surface fails nonuniformly, and it is corroded by single deep holes and pores.

In previous researches [42], a release of ions both of nickel and of titanium was observed; in the most acidic environment, the Ni released is about 1.5–2 times more (however, both concentrations are small, and the titanium concentration is not toxic for an organism), at pH 3.56 nickel concentration was 2–4 times more, and in other solutions titanium was not revealed which is consistent with literary data about its consumption on a passive film formation [8, 9, 42].

The ion concentrations of both nickel and titanium in solutions increase with time; however, this increase has a different character depending on the medium (**Figures 7** and **8**). During short-term tests [42], we believed that the slope of time-dependent concentration curves decreased gradually in all media, flattening out because of the termination of metal etching from the surface. It was so in general, however, the long-term investigation showed small

| Diameter, μm | Sample | pH |
|---|---|---|
| 280.00 | Nontreated | – |
| 280.00 | Annealed | – |
| 270.00 | Polished | – |
| 253.74 | Nontreated | 1.68 |
| 275.59 | Nontreated | 3.56 |
| 277.14 | Nontreated | 4.01 |
| 275.16 | Nontreated | 6.31/7.36 |
| 280.00 | Nontreated | 9.18 |
| 252.46 | Annealed | 1.68 |
| 257.00 | Polished | 1.68 |
| 270.03 | Nontreated | 1.5 (HCl) |

**Table 3.** Diameters of each type of NiTi wire sample before and after immersion for 2 years in solutions with various pH values.

fluctuations in the slope of the concentration curve toward increase and reduction of metal release in acid media. The last in comparison with published data can be related to sequential processes of the destruction and renewal of the protective oxide film (de- and repassivation) on defect areas [12, 44, 45].

The greater ion release from samples of a single type is observed in the most acidic medium (**Figure 8**), which abruptly drops with increasing pH and again increases in the NaCl solution. This corresponds to expectations. On the one hand, the metal ion release increases with increasing acidity, which in the theory corresponds to an increase in the corrosiveness of the medium. On the other hand, a high metal yield (it is greater than that for solution with acidity of 4.01 and 3.56 in the initial period and for pH 4.01 after 600 days) is revealed in the physiological saline, being a fairly concentrated source of chlorine ions, which are related to corrosion activator ions, having a depassivation and pitting corrosion effect, having a metal affinity greater than oxygen, and displacing the latter from its compounds with metals [46, 47].

Visually, the most damage occurs also at pH 1.68 after holding for 2 years (**Figure 9a** and **Table 3**). According to the location of pitting, the corrosive attack occurs coaxially to the direction of defects in production during drawing. Small traces of corrosion are observed at the surface at an acidity of 3.56. Defects of the metallic surface are no longer revealed at pH 4.01; however, depositions of organic nature are clearly expressed, which cover the wire with great strata and fibers but do not cover it completely (**Figure 9b**). Wires in the neutral solutions are covered by a smooth homogeneous surface layer (**Figure 9c**); and traces of pitting are absent, which supposedly is a result of repassivation of the damaged surface. Changes in the surface and diameter (**Table 3**) are not observed after holding in the alkaline medium. Because the used buffer solutions were not physiological media and served only for formation of the required pH, their effect on the alloy was compared with the effect of

hydrochloric acid [42]. The wire surface after long holding in HCl solution (**Figure 9d**) is more like the surface after holding in the physiological saline than in the acidic buffer, and the change in diameter (**Table 3**) is significantly less than that in a solution with pH 1.68. At the same time the concentrations of solved nickel for a short time in solutions of hydrochloric acid with pH 1.56 (the acidity changed to 2 after 2 years of immersion) and the buffer with pH 1.68 were close and that of titanium differed by more than a factor of two (after 10 days nickel concentration in HCl solution was 1.94 mg/l, titanium concentration was 0.515 mg/l). This gives occasion to suppose that the behavior mechanism in the two chloride-containing media is similar, etching of metals from the surface slows down at the initial similarity of magnitudes of solved nickel at long-term holding in the acid, and the surface is covered by a protective film.

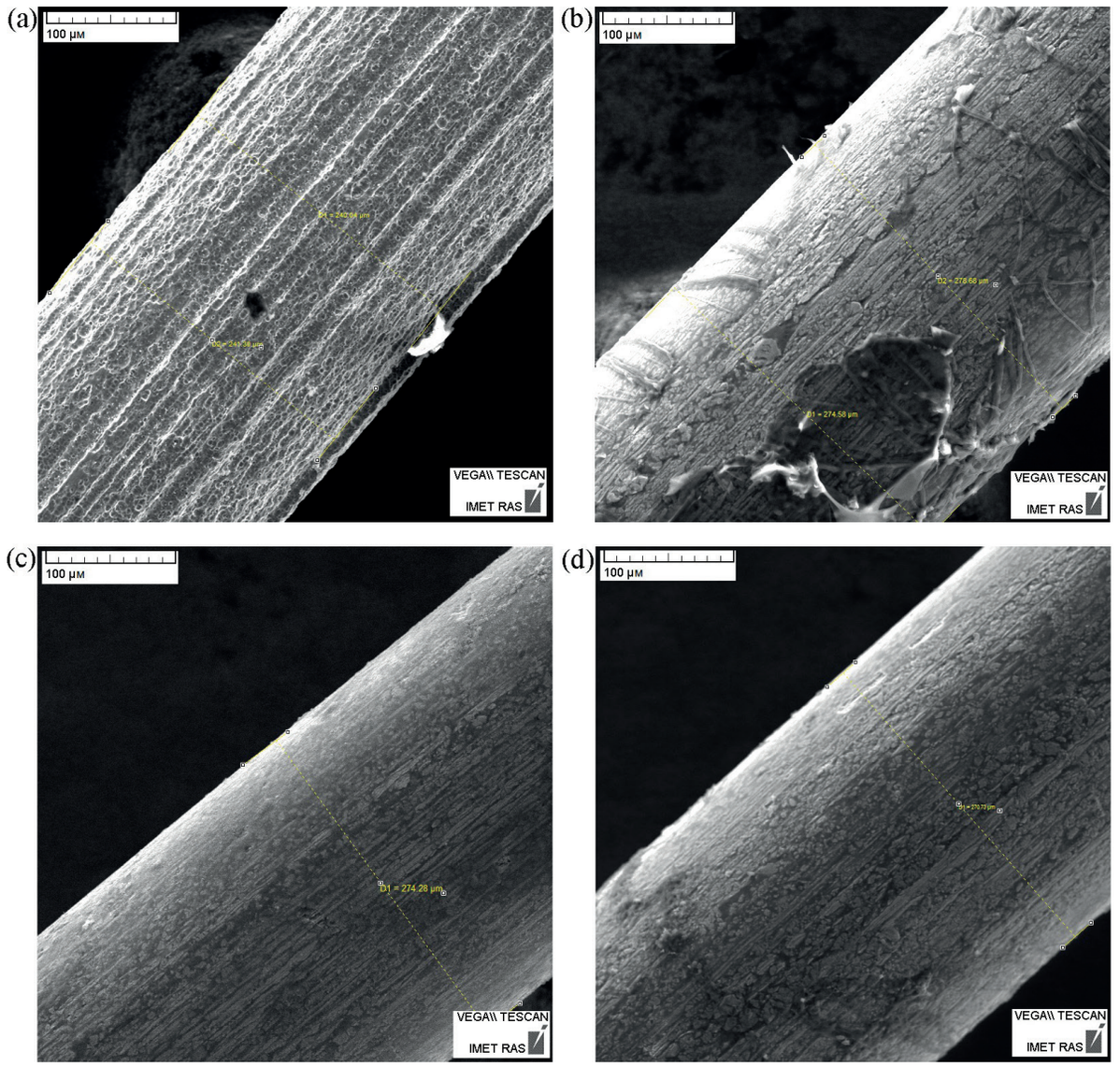


**Figure 9.** SEM image of the untreated NiTi sample surface after 2 years of immersion in various solutions: (a) buffer at pH 1.68 (Solution 1; **Table 2**); (b) buffer at pH 4.01 (Solution 3, **Table 2**); (c) 0.9 wt% NaCl (Solution 4, **Table 2**); and (d) HCl (pH 1.56).

In the case with solutions of salts of organic acids (pH 1.68–4.01), the dissolution of nickel and titanium is explained because both elements react with them [42]. In addition, regions of selective dissolution of metals were revealed, titanium in acidic media and nickel in acidic and neutral media [48]. However, nickel is subjected to corrosion damage in oxidizing media, and titanium is considered as satisfactorily stable (has a pitting corrosion potential almost two orders of magnitude higher than that for nickel in NaCl solution) [46, 47]. In addition, the investigation of the corrosion mechanism of microstructural nitinol in chlorine-containing solutions showed that the corrosive surface demonstrated a low content of nickel, and the result of the process was the Ni ion release into solution and the formation of titanium oxide in the damaged region because titanium remained at the surface and reacted with dissolved oxygen [12]. The region between volume NiTi and surface $TiO_2$ contained layers of $Ni_3Ti$ and $Ni_4Ti$ and clusters of pure nickel [1, 41, 11], the formation of which was caused also by the formation of the titanium oxide layer: nickel atoms are released from the Ni-Ti interatomic bond almost at room temperature when the thin oxide layer spontaneously forms at the nitinol surface, and nickel may be released into the solution. However, published data of the titanium ion release at the corrosion of microstructural nitinol were not found. Therefore, the presence of titanium ions in the NaCl solution turned out to be unexpected. Here, we suggest that this is related to the nanostructure of nitinol: nanograins failed during the "washout" of nickel from them and released a greater amount of titanium into the solution at the beginning [42]. Though titanium is not considered to be toxic for humans even in amounts much greater than those obtained here and its concentration in the solution is much less than the nickel content, it can be noted, however, that the nanostructural properties doubly affect the corrosion resistance of nitinol.

We observed that the significant retardation of the nickel ion release (and insignificant concentration as a whole) and the absence of titanium ion release form nanostructural nitinol samples in weakly acidic and neutral solutions after mechanical polishing. Traces of pitting corrosion on the surface of polished samples are visible only after 2 years of holding in the most acidic medium (**Figure 10**); wires held in the remaining media look intact equally. This leads to a conclusion of the occurrence of a strong and homogeneous protective surface layer

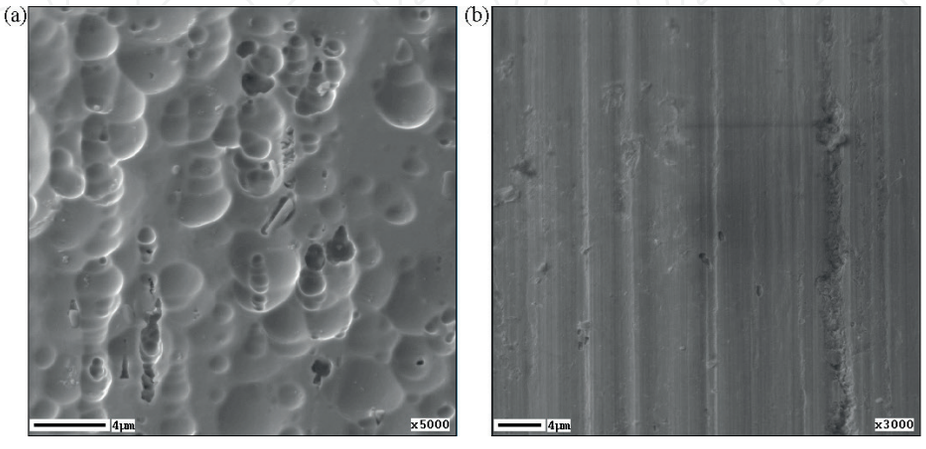


**Figure 10.** SEM image of the polished wire surface after holding in (a) solution with pH 1.68 and (b) remaining media.

of titanium oxide, which serves as a barrier to the release of nickel into the medium, and the high corrosion resistance of investigated nanostructural nitinol.

According to the literature, with increasing holding period of samples in the chlorine-containing solution, the thickness of the oxide layer increases [12, 14]. The investigation of untreated nitinol wires after 4 months of holding in the salt solution showed that their breakdown potential of the passive film changed from 200 to 800 mV, which the authors related to a decrease in the Ni content on the surface [17].

In this chapter, the surface composition of TiNi wires is practically invariable in the case with untreated and annealed samples after holding in solutions. Dark carbon-containing spots with insignificant nickel content and bright areas of titanium oxide with nickel inclusions, as before, alternate with each other, and the total analysis over an area of 100 × 100 μm² demonstrate the invariably high carbon content at a depth greater than 1 μm.

The greatest depth of the surface oxide layer, approximately 25 nm, is observed for polished wires after holding in neutral solutions (**Table 4**). At the same time, the titanium distribution in the elementary and bound states after the NaCl medium was determined, and elementary titanium was not revealed to a depth of 17 nm (**Figure 11**). The nickel contents at the surface

| **Solution pH** | **1.68** | **3.56** | **4.01** | **6.31/7.36** | **9.18** |
|---|---|---|---|---|---|
| Oxide layer thickness/nm | 8–13 | 13–17 | 15–20 | 23–28 | ≈10 |
| Nickel surface concentration/wt% | 8 | 5 | 3 | 0 | 3 |

**Table 4.** Surface composition of polished NiTi samples after immersion in various solutions for 2 years.

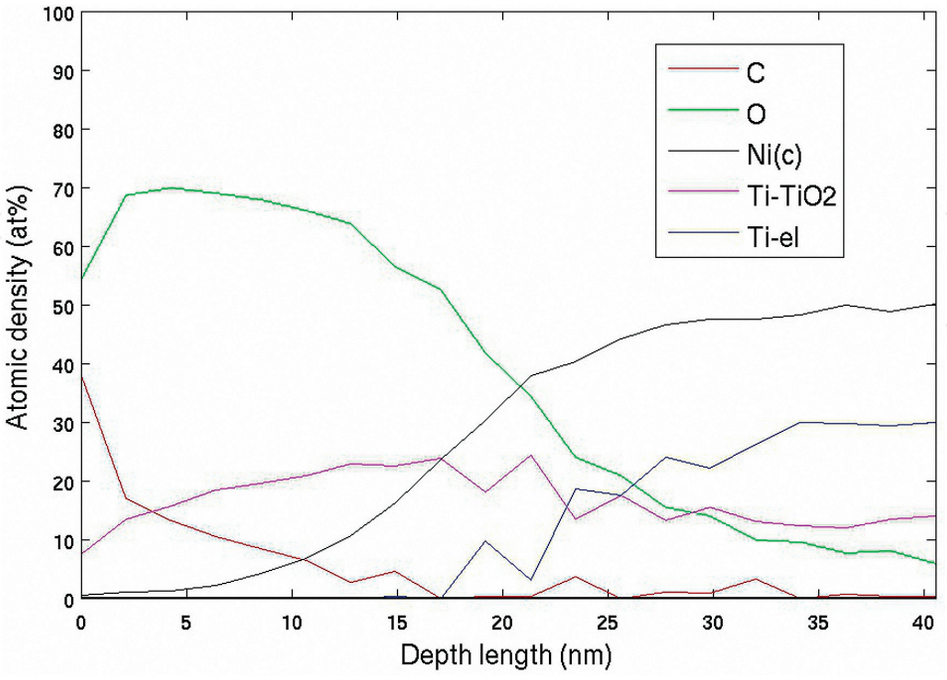


**Figure 11.** Composition of the polished NiTi wire surface after immersion for 2 years in 0.9 wt% NaCl (Solution 4, Table 2) as determined by Auger spectroscopy.

itself are shown in Table 4, in the NaCl and artificial plasma comes to a plateau at a depth of ≈20 nm, whereas in the remaining media, at about 10 nm. The oxygen concentration in the surface layer in all samples traverses the maximum at ≈60–70 wt% at a depth of 2.5–7 nm. At the same time, the carbon content on these dependences drops abruptly from a fairly high one at a depth to 2.5 nm, which can be related to the presence of outer mechanical contaminations at the surface. Release of metal ions into the solution with pH 9.18 was not observed completely, and this explains the identity of compositions before and after immersion.

Thus, the mechanically polished surface held in the chlorine-containing medium really looks protected from corrosion, including under dynamic conditions, even after subsequent annealing. However, the contact of nickel with the surrounding physiological environment nevertheless is possible that it demands to consider an individual susceptibility of patients.

The biocompatibility of the nanostructured nitinol was measured *in vitro* using standard test systems: the cultures of myofibroblasts from human peripheral vessels and human bone marrow mesenchymal stromal cells (MSC) were used as standard cell models. The myofibroblasts were isolated from cut peripheral veins [49] and grown in the DMEM medium (Biolot, Russia) with the addition of 10% fetal calf serum (Gibco, United States), 40 μg/mL of gentamicin at 37°C, and 5% carbon dioxide in a $CO_2$ incubator (Binder, Germany). The MSC (Biolot, Russia) were grown in the alpha-MEM medium (Sigma, United States) under the same conditions.

Samples of materials were placed into the wells of a 6-well plate (Greiner, Germany). Then cells were inoculated on the sample surface ($5 \times 10^3$ cells per $cm^2$) and cultured for 5 days. To determine the numbers of vital and dead cells, the cells growing on the material surface were stained with fluorescent dyes—acridine orange (Sigma, USA, 1 μg/mL) and propidium iodide (Sigma, USA, 1 μg/mL). Acridine orange stains both vital and dead cells, while propidium iodide stains only dead cells. After that, the samples were incubated for 10 min at 37°C [50]. Then the samples were examined under a DM 6000 fluorescence microscope (Leica, Germany). For the assay, at least 500 cells on the sample surface were counted. In the case of myofibroblasts and MSC, the percentages of vital cells for NiTi were 91 ± 3 and 95 ± 1, respectively. Thus, the material samples used in the study did not have a short-term toxic effect on the cells that overgrew its surfaces *de novo*.

The mitotic activity of the cells was assessed considering the mitotic index of the cells in the logarithmic growth phase (the 3rd day after inoculation). The number of mitotic cells was determined by fluorescence microscopy using the vital staining with the Hoechst 33342 fluorescent dye (Sigma, USA). The mitotic cells were identified based on the distribution of chromatin inherent in the prophase, metaphase, anaphase, and telophase. At least 500 cells on the sample surface were counted for the assay. The calculated MI value [51] for the cells growing on the NiTi surface was 3.1% for the myofibroblast culture and 1.8% for the MSC culture.

After 5 days of culturing, the morphological analysis of the myofibroblasts and MSC on the surface of material showed that myofibroblasts occupy only ≈75% of the NiTi surface accessible for the growth, while MSC occupy ≈50% of the accessible NiTi surface and so no monolayer is formed for either myofibroblasts or MSC.

This means that toxicity of samples was not revealed, but the cell reaction was not the best possible.

Thus it is shown that the use of nanostructured nitinol, obtained and investigated in this work, in medicine as a material for noninvasive implants is prospective compared with microstructured material, but formation of a corrosion-resistant and biocompatible surface layer in future still seems desirable.

Investigated nanostructural material is currently used to manufacture the noninvasive medical implants—stents—successfully applied to restore respiratory and urinary systems and esophageal and intestinal patency (**Figure 12**).

In connection with the presence of increased corrosion resistance, strength and plasticity, shape memory effect, controlled by the composition and heat treatment phase transformations, this

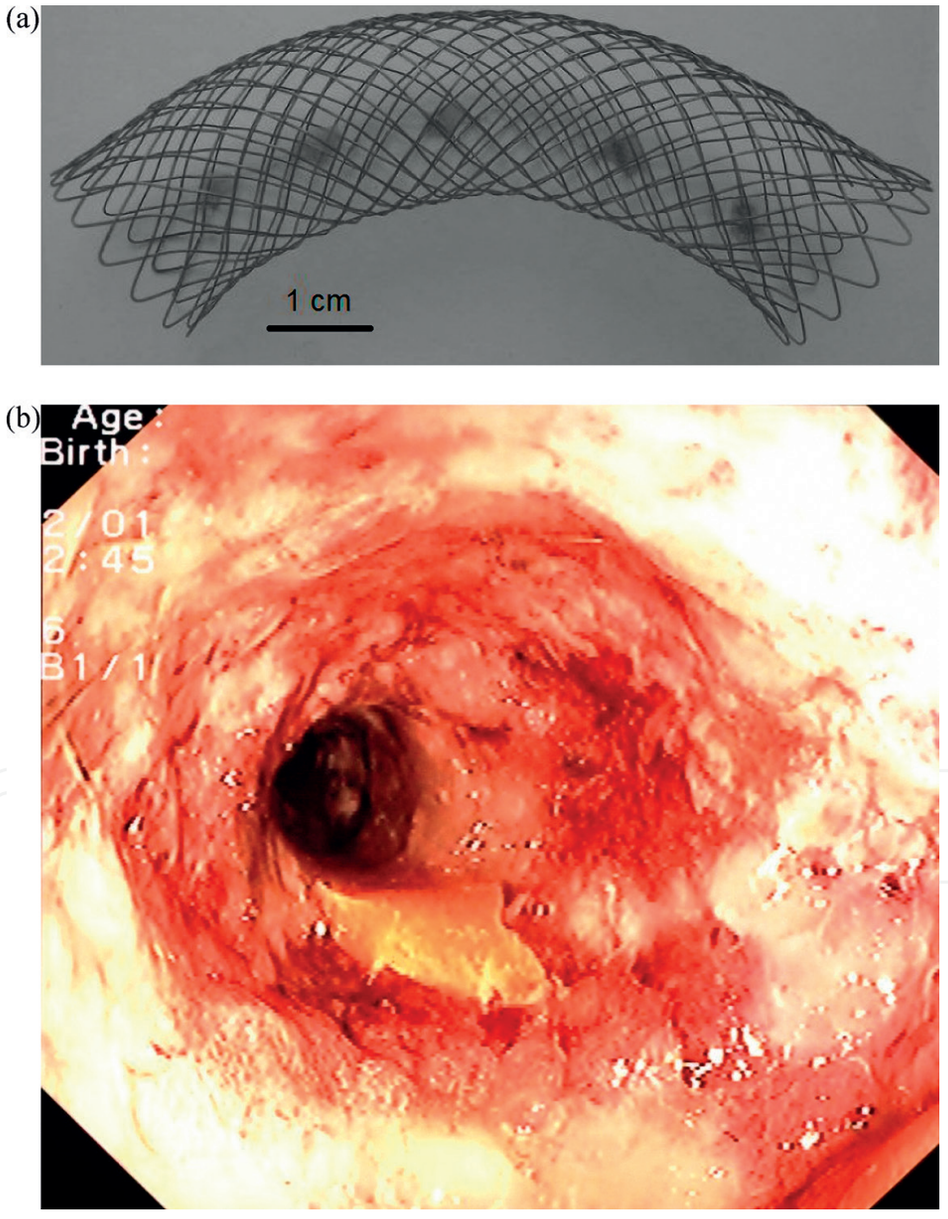


**Figure 12.** Patency restoration process: (a) stent applied to restore esophageal and intestinal patency, (b) example of the restoration of patency in the case of large intestine cancer via the implantation of a stent (operation and photo of the Blokhin Russian Cancer Research Center, Russian Academy of Medical Sciences).

new nanostructural material can also be used to create other medical products and instruments, as well as can be used in other areas that require the use of smart materials.

## 3. Conclusions

New nanostructural NiTi alloy that can be used in medical applications was obtained and investigated.

The material base is the B2 phase in the form of nanofibers with a diameter of 30–70 nm, which are elongated along the wire axis. Inclusions of $Ti_2Ni$ intermetallides are also observed, the distribution and the size of which are not affected by annealing at 450°C for 15 min.

The nickel release from investigated nanostructural nitinol is less in comparison with data for microstructural nitinol in a solution of any acidity. Although earlier in the literature, there were no similar results. Dissolution in the alkali medium is absent.

Mechanical treatment increases nitinol corrosion resistance, and thermal treatment decreases it, and the nanostructure possibly serves as the cause of the titanium ion presence in the solution of any acidity with unpolished samples. A significant retardation of the nickel ion release (and insignificant concentration as a whole) and the absence of titanium ion release in the weakly acidic and neutral solutions with polished samples are observed.

The mechanical treatment of the surface results in the formation of a thin layer of titanium oxide, decreases the roughness and number of defects but does not completely remove nickel from the surface. The nickel-free surface with the 25-nm titanium oxide protective layer is attained by holding in a neutral 0.9 wt% solution of sodium chloride. Such a layer must be the barrier to nickel release into the medium even under dynamic conditions.

A simultaneous 7–11% increase in strength and plasticity in comparison with microstructural nitinol was attained. The presence of the shape memory effect and the absence of an uncontrolled change in the temperature of phase transformations in connection with nanostructuring were noted.

Toxicity of samples has not been revealed. But no cell monolayer is formed on the surface of nanostructural alloy after 5 days of culturing of the myofibroblasts and mesenchymal stromal cells.

Nanostructured nitinol usage in medicine as a material for noninvasive implants is prospective compared with microstructured material but formation of corrosion-resistant and biocompatible surface layer still seems desirable.

## Acknowledgements

This work was supported by the RFBR № 15-33-70006 «mol_a_mos» and 14-29-10208 «ofi_m». The authors wish to thank Golberg MA, Dyomin K Yu, Mikhailova AB, Volchenkova VA, and Kargin Yu F for their help in sample analysis.

## Author details

Elena O. Nasakina*, Mikhail A. Sevostyanov, Alexander S. Baikin, Alexey V. Seryogin, Sergey V. Konushkin, Konstantin V. Sergienko, Alexander V. Leonov and Alexey G. Kolmakov

*Address all correspondence to: nacakina@mail.ru

A.A. Baikov Institute of Metallurgy and Material, Science, Russian Academy of Sciences, Moscow, Russia

## References

[1] Shabalovskaya S. On the nature of the biocompatibility and medical applications of NiTi shape memory and superelastic alloys. Bio-Medical Materials and Engineering. 1996;**6**:267-289. DOI: 10.3233/BME-1996-6405

[2] Gyunter VO, Khodorenko VN, Yasenchuk YF, Chekalkin TL. Nikelid titana. Meditsinskii material novogo pokoleniya (Titanium Nickelide. Medical Material of New Generation). Tomsk: MITs; 2006. p. 296

[3] Dotter CT, Buschmann PAC, McKinney MK, Rosch J. Transluminal expandable nitinol coil stent grafting: Preliminary report. Radiology. 1983;**147**:259-260. DOI: 10.1007/s00330-003-2022-5

[4] Zabolotnyi VT, Belousov OK, Palii NA, Goncharenko BA, Armaderova EA, Sevost'yanov MA. Materials science of the production, treatment and properties of titanium nickelide for application in endovascular surgery. Russian Metallurgy (Metally). 2011;**3**:437-448. DOI: 10.1134/S003602951105017X

[5] Stoeckel D. Nitinol medical devices and implants. Minimally Invasive Therapy & Allied Technologies. 2000;**9**:81-88

[6] Bose A, Hartmann M, Henkes HA. Novel. Self-expanding nitinol stent in medically refractory intracranial atherosclerotic stenosis: Wingspan study. Stroke. 2007;**38**:1531-1537. DOI: 10.1161/STROKEAHA.106.477711

[7] Xiaoying Lu, Xiang Bao, Yan Huang, Yinghua Qu, Huiqin Lu, Zuhong Lu. Mechanisms of cytotoxicity of nickel ions based on gene expression profiles. Biomaterials. 2009;**30**:141-148. DOI:10.1016/j.biomaterials.2008.09.011

[8] Nasakina EO, Sevostyanov MA, Goncharenko BA, Leonova YO, Kolmakov AG, Zabolotny VT. Metody issledovaniya I povysheniya korrozionnoy stoykosty meditsynskogo splava s effektom pamiaty formy NiTi. Issledovanie korrosionnoy stoykosty I biosovmestimosty nitinola [Methods of corrosion resistance research and increase of medical alloy with shape memory effect NiTi. Research of corrosion resistance and biocompatibility of nitinol]. Perspektivnie materialy [Advanced materials]. 2014;**7**:37-49

[9] Nasakina EO, Sevostyanov MA, Goncharenko BA, Leonova YO, Kolmakov AG, Zabolotny VT. Metody issledovaniya I povysheniya korrozionnoy stoykosty medit-synskogo splava s effektom pamiaty formy NiTi. Sposoby izmeneniya korrozionnoy stoykosti nitinola [Methods of corrosion resistance research and increase of medical alloy with shape memory effect NiTi. Ways of a nitinol corrosion resistance change]. Perspektivnie materialy [Advanced materials]. 2014;**9**:19-33

[10] Wever DJ, Veldhuizen AG, de Vries J, Busscher HJ, Uges DRA, van Horn JR. Electrochemical and surface characterization of a nickel-titanium alloy. Biomaterials. 1998;**19**: 761-769. DOI: 10.1016/S0142-9612(97)00210-X

[11] Shabalovskaya SA., Tian He, Anderegg JW, Schryvers DU, Carroll WU, Van Humbeeck J. The influence of surface oxides on the distribution and release of nickel from Nitinol wires. Biomaterials. 2009;**30**(4):468-477. DOI: 10.1016/j.biomaterials.2008.10.014

[12] Hu T, Chu C, Xin Y, Wu S, Yeung KWK, Chu PK. Corrosion products and mechanism on NiTi shape memory alloy in physiological environment. Journal of Materials Research. 2010;**25**:350-358. DOI: 10.1557/JMR.2010.0051

[13] Trepanier C, Venugopalan R, Messer R, Zimmerman J, Pelton AR. Effect of passivation treatments on nickel release from nitinol. In: Proceedings of the 6th World Biomaterials Congress Transactions; 2000; Honolulu. Minneapolis: Society for Biomaterials; 2000. p. 1043

[14] Barrett RD, Bishara SE, Quinn JK. Biodegradation of orthodontic appliances: Part I. Biodegradation of nickel and chromium in vitro. American Journal of Orthodontics and Dentofacial Orthopedics. 1993;**103**:8-14. DOI:10.1016/0889-5406(93)70098-9

[15] Her-Hsiung Huang, Yu-Hui Chiu, Tzu-Hsin Lee, Shih-Ching Wu, Hui-Wen Yang, Kuo-Hsiung Su, Chii-Chih Hsu. Ion release from NiTi orthodontic wires in artificial saliva with various acidities. Biomaterials. 2003;**24**:3585-3592. DOI: 10.1016/S0142-9612(03)00188-1

[16] Uo M, Watari F, Yokoyama A, Matsuno H, Kawasaki T. Dissolution of nickel and tissue response observed by Xray scanning analytical microscopy. Biomaterials. 1999;**20**:747-755. DOI: 10.1016/S0142-9612(98)00224-5

[17] Clarke B, Kingshott P, Hou X, Rochev Y, Gorelov A, Carroll W. Effect of nitinol wire surface properties on albumin adsorption. Acta Biomaterialia. 2007;**3**:103-111. DOI: 10.1016/j.actbio.2006.07.006

[18] Her-Hsiung Huang. Surface characterizations and corrosion resistance of nickel–titanium orthodontic archwires in artificial saliva of various degrees of acidity. Journal of Biomedical Materials Research Part A. 2005;**74A**:629-639. DOI: 10.1002/jbm.a.30340

[19] Shabalovskaya SA, Anderegg J, Wataha J, Adler P, Cunnick J. Effects of surface chemistry on biocompatibility of NiTi. In: Proceedings of the International Conference on Shape Memory and Superelastic Technologies; October 3-7, 2004; Kurhaus Baden-Baden. Materials Park: ASM International; 2004. pp. 367-375

[20] Her-Hsiung Huang. Variation in corrosion resistance of nickel-titanium wires from different manufacturers. Angle Orthodontist. 2005;**75**:661-665

[21] Trepanier C, Tabizian M, Yahia LH, Bilodeau L, Piron DL. Effect of modification of oxide layer on NiTi stent corrosion resistance. Journal of Biomedical Materials Research. 1998;43:433-440

[22] Trepanier C, Fino J, Zhu L, Pelton AR. Corrosion resistance of oxidized nitinol. In: Proceedings of the International Conference on Shape Memory and Superelastic Technologies. SMST-2003; 5-8 May 2003; California. California: SMST Soc; 2004. pp. 267-276

[23] Farrukh MA, editor. Functionalized Nanomaterials. Rijeka: InTech; 2016. pp. 172. DOI: 10.5772/63186

[24] Roldugin VI, Fedotov MA, Folmanis GE, Kovalenko LV, Tananaev IG. Formation of aqueous colloidal solutions of selenium and silicon by laser ablation. Doklady Physical Chemistry. 2015;**463**:161-164. DOI: 10.1134/S0012501615070064

[25] Leon Mishnaevsky Jr., Levashov E, Ruslan Z, Valiev, Javier Segurado, Ilchat Sabirov, Nariman Enikeev, Sergey Prokoshkin, Andrey V Solov'yov, Andrey Korotitskiy, Elazar Gutmanas, Irene Gotman, Eugen Rabkin, Sergey Psakh'e, Luděk Dluhoš, Marc Seefeldt, Alexey Smolin. Nanostructured titanium-based materials for medical implants: Modeling and development. Materials Science and Engineering R. 2014;**81**:1-19. DOI: 10.1016/j.mser.2014.04.002

[26] Amirhanova NA, Valiev RZ, Adasheva SL, Prokof'ev EA. Issledovanie korrozionnyh i jelektrohimicheskih svojstv splavov na osnove nikelida titana v krupnozernistom i ul'tramelkozernistom sostojanijah [Investigation of corrosion and electrochemical properties of alloys based on nickel titanium in coarse and ultrafine states]. Journal of the Ufa State Aviation Technical University. 2006;**7**(1):143-146

[27] Korotin DM, Bartkowski S, Kurmaev EZ, Cholakh SO, Müller M, Neumann M, Gunderov D, Valiev RZ, Cholakh SO. Arsenic contamination of coarse-grained and nanostructured nitinol surfaces induced by chemical treatment in hydrofluoric acid. Journal of Biomedical Materials Research Part B: Applied Biomaterials. 2012;**100B**(7):1812-1816. DOI: 10.1002/jbm.b.32748

[28] Zheng CY, Nie FL, Zheng YF, Cheng Y, Wei SC, Valiev RZ. Enhanced in vitro biocompatibility of ultrafine-grained titanium with hierarchical porous surface. Applied Surface Science. 2011;**257**(13):5634-5640. DOI: 10.1016/j.apsusc.2011.01.062

[29] Zheng CY, Nie FL, Zheng YF, Cheng Y, Wei CS, Liqun Ruan, Valiev RZ. Enhanced corrosion resistance and cellular behavior of ultrafine-grained biomedical NiTi alloy with a novel SrO-$SiO_2$-$TiO_2$ sol-gel coating. Applied Surface Science. 2011;**257**(13):5913-5918. DOI: 10.1016/j.apsusc.2011.02.006

[30] Zhang XN. Biomechanical and biocorrosion properties of nanostructured titanium. Advanced Materials Research. 2007;**29-30**:51-54. DOI: 10.4028/www.scientific.net/AMR.29-30.51

[31] Aslan Ahadi, Qingping Sun. Effects of grain size on the rate-dependent thermomechanical responses of nanostructured superelastic NiTi. Acta Materialia. 2014;**76**:186-197. DOI: 10.1016/j.actamat.2014.05.007

[32] Delville R, Malard B, Pilch J, Sittner P, Schryvers D. Transmission electron microscopy study of dislocation slip activity during superelastic cycling of NiTi. International Journal of Plasticity. 2010;**27**:282-297. DOI: 10.1016/j.ijplas.2010.05.005

[33] Shu-yong Jiang, Ya-nan Zhao, Yan-qiu Zhang, Ming Tang, Chun-feng LI. Equal channel angular extrusion of NiTi shape memory alloy tube. Transactions of Nonferrous Metals Society of China. 2013;**23**:2021-2028. DOI: 10.1016/S1003-6326(13)62691-6

[34] Zhilyaev AP, Langdon TG. Using high-pressure torsion for metal processing: Fundamentals and applications. Progress in Materials Science. 2008;**53**:893-979. DOI: 10.1016/j.pmatsci.2008.03.002

[35] Stolyarov VV. Deformability and nanostructuring of TiNi shape-memory alloys during electroplastic rolling. Materials Science and Engineering A. 2009;**503**:18-20. DOI: 10.1016/j.msea.2008.01.094

[36] Liu HS, Mishnaevsky Jr L. Martensitic transformations in nanostructured nitinol: Finite element modeling of grain size and distribution effects. Computational Materials Science. 2013;**76**:27-36. DOI: 10.1016/j.commatsci.2012.11.032

[37] Adharapurapu RR, Vecchio KS. Effects of aging and cooling rate on the transformation of nanostructured Ti-50.8Ni. Journal of Alloys and Compounds. 2017;**693**:150-163. DOI: 10.1016/j.jallcom.2016.09.112

[38] Vojtech D, Michalcová A, Capek J, Marek I, Dragounová L. Structural and mechanical stability of the nano-crystalline Ni-Ti (50.9 at.% Ni) shape memory alloy during short-term heat treatments. Intermetallics. 2014;**49**:7-13. DOI: 10.1016/j.intermet.2013.12.013

[39] Divya Rani VV, Vinoth-Kumar L, Anitha VC, Manzoor K, Deepthy M, Nair Shantikumar V. Osteointegration of titanium implant is sensitive to specific nanostructure morphology. Acta Biomaterialia. 2012;**8**:1976-1989. DOI: 10.1016/j.actbio.2012.01.021

[40] Shishkovsky I, Morozov Yu., Smurov I. Nanofractal surface structure under laser sintering of titanium and nitinol for bone tissue engineering. Applied Surface Science. 2007;**254**:1145-1149. DOI:10.1016/j.apsusc.2007.09.021

[41] Zhu L, Trepanier C, Fino J, Pelton AR. Oxidation of nitinol and its effect on corrosion resistance. In: Proceedings of the Conference on ASM Matererials. Proceedings for Medical Device; 2003; Anaheim. Materials Park, Cleveland: ASM International; 2004. pp. 8-10

[42] Nasakina EO, Baikin AS, Sevost'yanov MA, Kolmakov AG, Zabolotnyi VT, Solntsev KA. Properties of nanostructured titanium nickelide and composite based on it. Theoretical Foundations of Chemical Engineering. 2014;**48**(4):477-486. DOI: 10.1134/S0040579514040071

[43] Tomic S, Rudolf R, Brun ko M, Anžel I, Savic V, Olic M. Response of monocytederived dendritic cells to rapidly solidified nickeltitanium ribbons with shape memory properties. European Cells & Materials. 2012;**23**:58-81. DOI: 10.22203/eCM.v023a05

[44] Venugopalan R, Trepanier C. Assessing the corrosion behavior of nitinol for minimally-invasive device design. Minimally Invasive Therapy & Allied Technologies. 2000;**9**:67-74

[45] Sun EX, Fine S, Nowak WB. Electrochemical behavior of nitinol alloy in ringer's solution. Journal of Materials Science: Materials in Medicine. 2002;**13**:959-964. DOI: 10.1023/A:1019812729884

[46] Zhuk NP. Kurs korrozii i zashhity metallov [The course of corrosion and protection of metals]. Moscow: Metallurgy; 1976

[47] Ulig GG, Revi GU. Korrozija i bor'ba s nej. Vvedenie v korrozionnuju nauku i tehniku [Corrosion and its prevetion]. Leningrad: Chemestry; 1989

[48] Shcherbakov AI, Kasatkina IV, Zalavutdinov RK. Ustojchivost' splava «pamjati» TiNi k selektivnoj korrozii [Resistance of "Memory" alloy TiNi to selective corrosion]. Corrosion: Materials and Protection. 2007;**12**:14-16

[49] Akatov VC, Fadeeva IC, Chekanov AV, Solov'yev VV. Rol' kletok retsipiyenta v mekhanizme patologicheskoy kal'tsifikatsii transplantatov klapanov serdtsa i sosudov [Role of the recipient cells in the mechanism of transplants pathological calcification of heart valves and blood vessels]. Biofizika. 2010;**55:**937-942

[50] Garmash SA, Smirnova VS, Karp OE, Usacheva AM, Berezhnov AV, Ivanov VE, Chernikov AV, Bruskov VI, Gudkov SV. Pro-oxidative, genotoxic and cytotoxic properties of uranyl ions. Journal of Environmental Radioactivity. 2014;**127**:163-170. DOI: 10.1016/j.jenvrad.2012.12.009

[51] Permyakov SE, Knyazeva EL, Khasanova LM, Fadeev RS, Zhadan AP, Roche-Hakansson H, Håkansson AP, Akatov VS, Permyakov EA. Oleic acid is a key cytotoxic component of HAMLET-like complexes. Biological Chemistry. 2012;**393**:85-92